Available online at www.sciencedirect.com
ScienceDirect
Ceramics International 36 (2010) 1711–1717
CERAMICS INTERNATIONAL
www.elsevier.com/locate/ceramint

Short communication

Microstructure and refractory properties of spinel containing castables

Salah A. Abo-El-Enein [a,*], Morsy M. Abou-Sekkina [b], Nagy M. Khalil [c], Osama A. Shalma [d]

[a] Department of Chemistry, Faculty of Science, Ain Shams University, Cairo, Egypt
[b] Department of Chemistry, Faculty of Science, Tanta University, Tanta, Egypt
[c] Refractories, Ceramics and Building Materials Department, National Research Center (NRC), Giza, Egypt
[d] Environmental Monitoring Laboratory, Tanta, Egypt

Received 11 November 2009; received in revised form 17 December 2009; accepted 2 February 2010
Available online 9 March 2010

Abstract

The bauxite-based and kaolin-based refractory castables investigated were carefully prepared. They are composed of 90 wt.% well-graded (coarse, medium, and fine) bauxite or kaolin aggregates, 10 wt.% binding matrix and adequate amount of distilled water. The binder mixture was calcium aluminate cement (CAC) containing 80% alumina and magnesium-aluminate spinel (MA-spinel) either preformed or in situ. The castable batches were cast into cubes (25 mm × 25 mm × 25 mm), left at 100% relative humidity for 24 h cured for 7 days under water, and dried at 110 °C for 24 h. The samples were then subjected to firing at 1550 °C for a soaking time of 1 h.

The microstructure and refractory properties of the prepared castable samples were investigated by using X-ray diffraction (XRD) analysis, scanning electron microscopy (SEM), energy dispersive X-ray (EDX) analysis, permanent linear changes (PLC) test and refractoriness under load (RUL) test. The slag-attack resistance test was applied to determine the degree of penetration of slag and/or the rate of corrosion. The results of these investigations were related as much as possible to each other.

The investigated castable samples showed characteristic positive PLC and good volume stability (linear change <1%). They started softening at about 1300 °C followed by the rapid subsidence. They showed a somewhat decrease in penetration by the molten slag and a slight increase in corrosion as the spinel (preformed or in situ) content increases. The castable samples containing in situ spinel showed an increase in resistance to slag-penetration and a slightly higher corrosion due to slag attack compared to castable samples containing preformed spinel.

Keywords: Kaolin-based refractory; Spinel containing castables; Phase composition; Refractory properties

1. Introduction

Refractory castables or concretes are relatively new class of refractories. They have gained wide applications during the last decades. They offer various advantages over conventional refractory bricks in terms of application rate as well as cost and flexibility, making them attractive to all other industrial users.

Refractory castables consist in precision graded coarse and fine refractory grains. They are gelled by means of a binder system in the materials green state. Following the heat-up of the material, the binder either transforms or volatilizes, facilitating the formation of a ceramic bond. The most common binder used in castables is calcium aluminate cement (CAC). Castables are mixed with water and then installed by either pouring or pumping. They acquire high mechanical strength at high temperatures and further improvements in properties occur after firing. They are resistant to high temperatures, mechanical stress, thermal stress, chemical and abrasive attack. They are largely dependent upon the choice of refractory aggregate and hydraulic cement used; thus a wide variety of aggregates and several types of cements could be used to produce a lot of refractory concrete products with markedly different properties. The quality of refractory concrete is improved through decreasing the cement content, i.e. 4–8% in low cement castables (LCC) or 1–3% in ultra low cement castables (ULCC) [1] or <1% in zero cement castables (ZCC). The LCC, ULCC and ZCC have replaced many conventional castables, plastics, ramming and gunning mixes. These concretes develop very high performance at heat and after heating. They are used extensively in refractory applications due to their excellent properties and ease of installation [2]. They are used when thermal shock resistance or resistance against abrasion and corrosion by slags or melting metals is required.

* Corresponding author.
E-mail address: saaboelenein@yahoo.com (S.A. Abo-El-Enein).

0272-8842/$36.00
doi:10.1016/j.ceramint.2010.02.015

MA-spinel ($MgAl_2O_4$) is a very desirable phase in castables where improved hot strength, creep resistance, good thermal stability and slag penetration resistance are required [3].

In the present work, the phase composition and microstructure of bauxite-based or kaolin-based refractory castables containing spinel (preformed or in situ) were investigated by X-ray diffraction analysis (XRD), and scanning electron microscopy (SEM). A comparative study was done between these two types of refractory castables with respect to permanent linear change (PLC), refractoriness under load (RUL) and slag-attack resistance, in order to evaluate their refractory properties.

2. Experimental procedures

The starting materials used in this investigation are: calcium aluminate cement (Alcoa, CA-25R-80% alumina), Chinese calcined bauxite aggregate, Egyptian kaolin aggregate, preformed MA-spinel ($MgAl_2O_4$), magnesium oxide ''MgO'' (BDH) and aluminum oxide ''Al_2O_3'' (Alcoa).

The refractory aggregates (calcined bauxite or kaolin) were well graded as 65 wt.% coarse (2.36–0.50 mm), 10 wt.% medium (0.50–0.25 mm) and 25 wt.% fine (<0.25 mm). The refractory castable samples were prepared according to the compositions represented in Tables 1 and 2, where a 90 wt.% well-graded aggregate intermixed with the binding matrix and adequate amounts of distilled water according to the standard ''good ball in hand'' ASTM C-860 method. The mixed batches were then cast into cubes of 25 mm side length in steel moulds and left in their moulds at 100% relative humidity for 24 h. The samples were then demoulded and further cured for 7 days under water, and dried at 110 °C for 24 h. Finally the samples were subjected to firing at 1550 °C in an electric muffle furnace for a soaking time of 1 h.

The refractory castable samples were characterized using X-ray diffraction (XRD) analysis and scanning electron microscopy (SEM). The permanent linear change (PLC) was measured in terms of expansion or contraction percentage after firing the cubic castable specimens at 1550 °C for 2 h. RUL test was carried out according to DIN Standard No. 1893 (1983) using the Tonindustrie type apparatus, to measure the resistance the castable samples to the combined effect of heat and loading. The crucible test was performed to determine the slag-attack resistance of the investigated refractory castable specimens where the prefired (at 1550 °C for 1 h) castable cubes were drilled at the center in order to make cylindrical grooves and then the grooves were filled up with the slag. The cubes were fired at 1350 °C for 2 h. The cubes were then removed, cooled, sectioned, photographed and the slag/refractory interface was examined. SEM and EDX of B2 and K2 castable samples were performed to indicate the interaction of preformed spinel in the castable samples. A ''JEOL JXA-840'' high resolution scanning electron microscope was used.

Table 1
Mix composition of refractory castable batches based on calcined bauxite aggregate (B).

Sample symbol	Bauxite aggregate (wt.%)	Binding matrices		
		CAC (wt.%)	Spinel (wt.%)	
B0	90	10	0	
B1	90	8	2	Preformed spinel
B2	90	6	4	
B3	90	4	6	
B7	90	8	2	In situ spinel
B8	90	6	4	($MgO + Al_2O_3$)
B9	90	4	6	

Table 2
Mix composition of refractory castable batches based on kaolin aggregate (K).

Sample symbol	Kaolin aggregate (wt.%)	Binding matrices		
		CAC (wt.%)	Spinel (wt.%)	
K0	90	10	0	
K1	90	8	2	Preformed spinel
K2	90	6	4	
K3	90	4	6	
K7	90	8	2	In situ spinel
K8	90	6	4	($MgO + Al_2O_3$)
K9	90	4	6	

3. Results and discussion

3.1. Microstructure of the fired castables

The phase composition of the bauxite-based (B0, B2 and B8) and kaolin-based (K0, K2 and K8) castable specimens, sintered at 1550 °C for 1 h, were investigated by means of X-ray diffraction (XRD) analysis and scanning electron microscopy (SEM). The castable specimen B0 was taken as the control castable sample for bauxite-based castables. XRD patterns of the castable specimens B0, B2 and B8 are shown in Fig. 1. The XRD patterns indicated the formation of the corundum phase along with mullite phase for all of the three castable specimens. The other minor phases, CAC and spinel or its oxides, cannot be detected by XRD analysis. The SEM micrographs of the castable specimens B2 and B8 are shown in Figs. 2 and 3. The mineral phases of bauxite castable samples are essentially corundum, mullite, and glass. Their microstructure is mainly composed of granular corundum skeleton structure interlaced with mullite crystals; similar observations were also reported in an earlier investigation [4]. The SEM micrographs show densely packed microstructures with an abundant of corundum grains of comparable sizes, rounded and sub-rounded, homogeneously embedded in the matrix. Some needle-shaped (elongated rod) mullite crystals are also distributed from place to place. The liquid phase could also be distinguished in the matrix due to the impurities and calcium aluminate cement present in the bauxite castables; similar results were obtained in earlier publications [3,5,6]. Grain shapes vary from spherical to polyhedral nature and some pores are trapped inside the grains [3]. The corundum phase appeared due to the transformation of bauxite minerals to corundum. This transformation occurred in

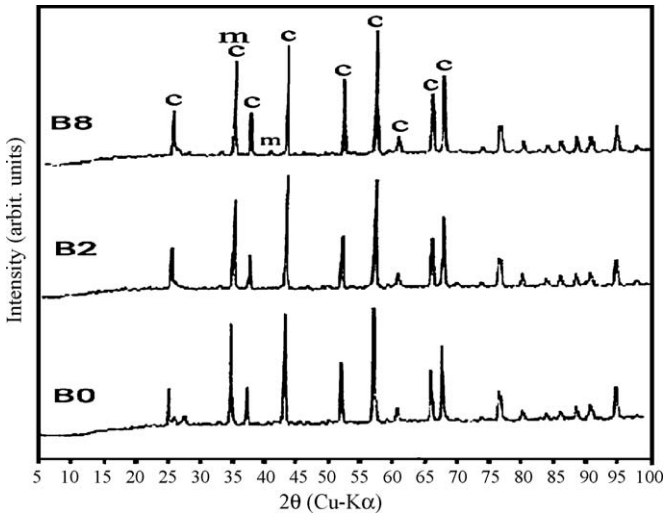

Fig. 1. X-ray diffraction patterns of castables B0, B2 and B8 fired at 1550 °C for 1 h (c: corundum, m: mullite).

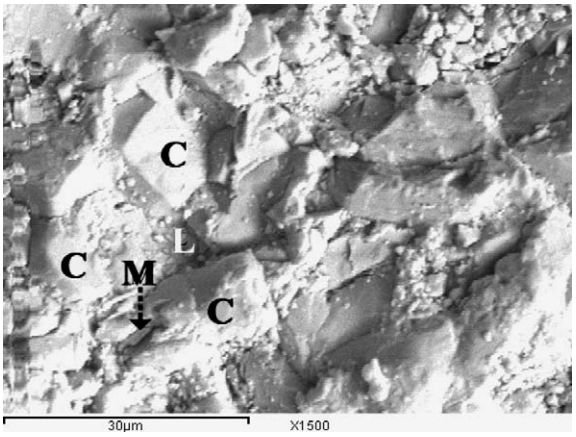

Fig. 2. SEM photomicrographs of B2 castable sample fired at 1550 °C for 1 h (C: corundum grains, M: needle-shaped mullite, L: liquid phase).

two distinct steps, namely: (i) the dehydroxylation (at about 500 °C) leads to the formation of the transition phase and (ii) a sort of localized atomic rearrangement in which the tetrahedrally coordinated Al in the α-Al_2O_3 structure move to

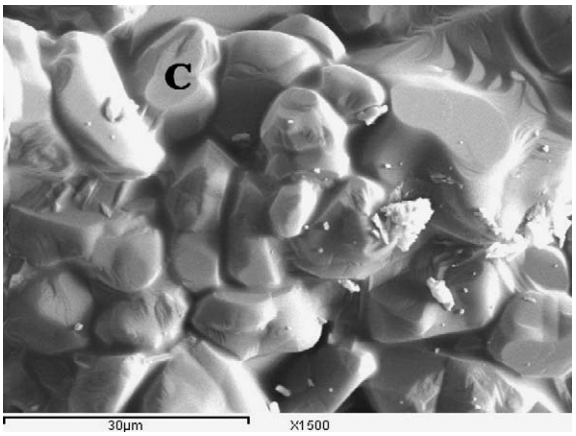

Fig. 3. SEM photomicrographs of B8 castable sample fired at 1550 °C for 1 h (C: corundum grains).

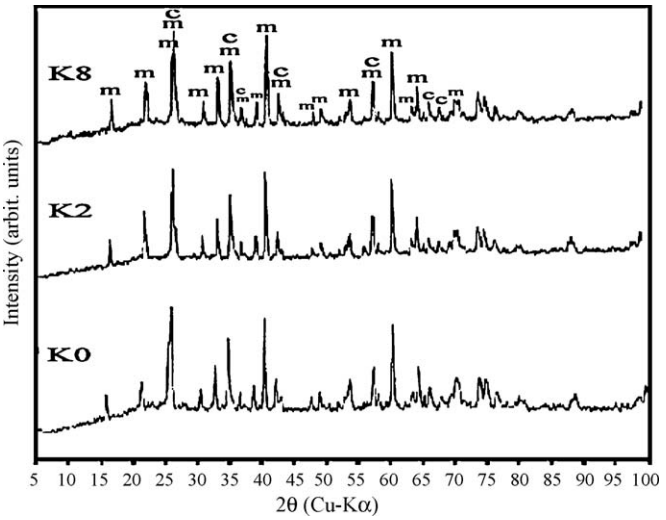

Fig. 4. X-ray diffraction patterns of castables K0, K2 and K8 fired at 1550 °C for 1 h (c: corundum, m: mullite).

octahedrally coordinated sites in the corundum structure [7]. The presence of different impurities in bauxite versus alumina helps the formation of mullite that appeared as a result of the reaction between silica impurities and alumina in the castable samples sintered at 1550 °C [6].

The XRD patterns of the kaolin-based castable specimens K0, K2 and K8 are shown in Fig. 4. The castable sample K0 was considered as the control castable sample. The XRD patterns indicated that all the castable specimens are composed mainly of transformed mullite phase along with some peaks characterizing the corundum phase. Other minor phases, CAC and spinel (preformed or in situ), present in small quantities and could not be detected by XRD analysis. The SEM micrographs of the kaolin-based castable specimens K2 and K8 are shown in Figs. 5 and 6. They show that the kaolin particles are usually stacked together to form agglomerates, and the irregular Al_2O_3 particles are dispersed in the matrix. The primary mullite appears to grow from the kaolin raw materials with a rod-like shape [8]. Mullite and corundum phases appeared as a result of sintering of castable samples at 1550 °C

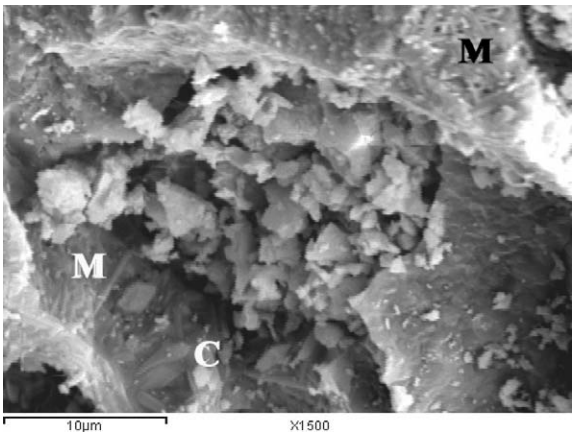

Fig. 5. SEM photomicrographs of K2 castable sample fired at 1550 °C for 1 h (C: corundum grains, M: needle-shaped mullite).

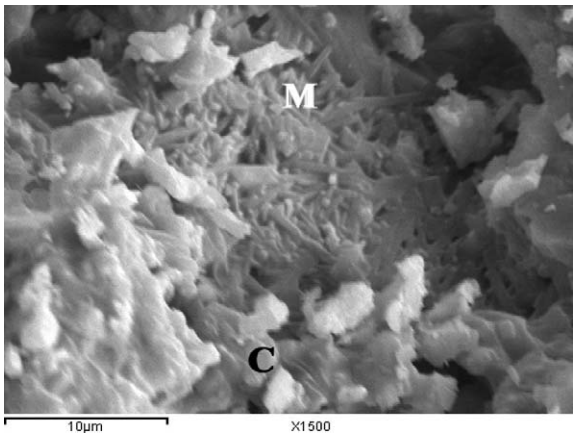

Fig. 6. SEM photomicrographs of K8 castable sample fired at 1550 °C for 1 h (C: corundum grains, M: needle-shaped mullite).

for 1 h where kaolinite ($A1_2O_3{\cdot}2SiO_2{\cdot}2H_2O$), the essential component of kaolin, lost the OH units in its crystal structure at around 450 °C, forming an almost amorphous material known as metakaolinite ($Al_2O_3{\cdot}2SiO_2$). Metakaolinite structure is unstable and, at about 1000 °C, is transformed to γ-alumina, cristoballite (SiO_2) and primary mullite crystals. At higher temperatures, the crystals of primary mullite grow by reacting with amorphous aluminosilicate phase forming secondary mullite [9,10]. The impurities distort the atomic structure and assist the formation of liquid phase at higher firing temperatures.

3.2. Refractory properties

3.2.1. Permanent linear change (PLC)

The results of permanent linear changes of the castable specimens are tabulated in Tables 3 and 4 for bauxite-based and kaolin-based specimens, respectively. The investigated castable samples showed good volume stability as it indicated a very small linear change.

The castable samples containing alumina and magnesia show characteristic expansion when spinel is being formed as confirmed by Myhre et al. [11]. The in situ spinel formation leads to two significant disadvantages which degrade the properties of the castable specimens containing in situ spinel compared to those containing preformed spinel; firstly, a lot of volatiles are released [3,12,13], which generate micro-bubbles in the castable leading to a more porous structure and secondly, the in situ spinel formation is associated with a considerable volume expansion [13,14].

3.2.2. Refractoriness under load

Two bauxite-based castable samples, B2 and B8, were selected in order to investigate the RUL and the results are shown in Fig. 7.

For the castable sample B2, Fig. 7, the maximum thermal expansion of 0.942% was reached at a temperature (T_0) of 1250 °C. Once the maximum expansion is reached, the castable sample started to significantly deform with further increase in temperature. At a temperature of 1300 °C, the expansion value

Table 3
Permanent linear change (PLC) (%) of the bauxite-based castable samples.

Castable	Bauxite aggregate (wt.%)	Binding matrices			Permanent linear change (PLC) (%)
		CAC (wt.%)	Spinel (wt.%)		
B0	90	10	0		0.125
B1	90	8	2	Preformed	0.145
B2	90	6	4		0.146
B3	90	4	6		0.149
B7	90	8	2	In situ	0.158
B8	90	6	4		0.161
B9	90	4	6		0.167

Table 4
Permanent linear change (PLC) (%) of the kaolin-based castable samples.

Castable	Kaolin aggregate (wt.%)	Binding matrices			Permanent linear change (PLC) (%)
		CAC (wt.%)	Spinel (wt.%)		
K0	90	10	0		0.101
K1	90	8	2	Preformed	0.120
K2	90	6	4		0.125
K3	90	4	6		0.125
K7	90	8	2	In situ	0.199
K8	90	6	4		0.199
K9	90	4	6		0.200

decreased to 0.850%. With further heating to higher temperatures up to 1500 °C, the deformation of the castable sample continued till reach the contraction value −1.133% at 1450 °C where the castable sample collapsed. At temperatures around 1200 °C, the strength of the castable sample B2 drops significantly, probably due to more liquid phase formation, which influenced the grain boundary sliding motion [15,16]. The softening temperature (T_a) of the loaded castable sample was found to be 1386 °C.

Fig. 7 represents the deformation under load of the castable sample B8. A maximum thermal expansion of 0.860% was attained at a temperature (T_0) of 1200 °C. On further increase in temperature, the castable sample started to deform significantly. A noticeable decrease in the thermal expansion value is observed as the temperature increases. At a temperature of

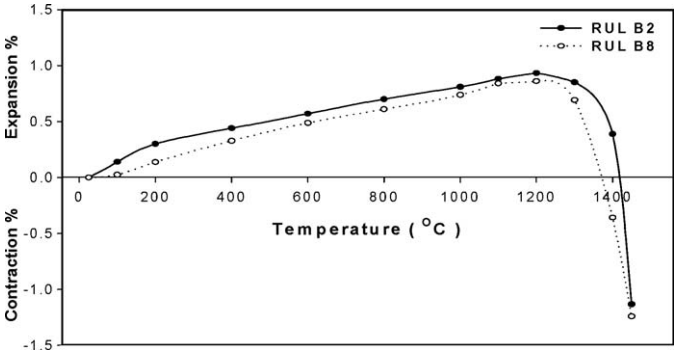

Fig. 7. RUL curves of B2 and B8 (prefired at 1550 °C for 1 h).

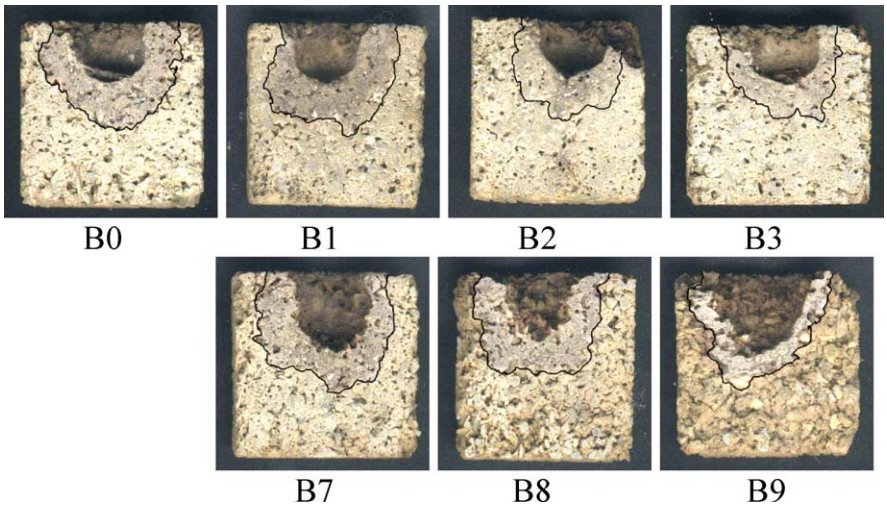

Fig. 8. Photographed sections of slag-corrosion and slag-penetration in bauxite-based castable samples (B0, B1, B2, B3, B7, B8 and B9).

Table 5
Chemical composition of granulated blast-furnace slag (GBFS).

Content	%	Content	%	Content	%
CaO	35.62	MgO	2.68	S^{2-}	0.54
SiO_2	34.97	Na_2O	1.34	SO_3^-	0.15
Al_2O_3	11.42	K_2O	0.56	Cl^-	0.01
BaO	6.37	TiO_2	0.44	–	–
Mn_2O_3	5.62	P_2O_5	0.07	–	–

1250 °C, the expansion value decreases to 0.799%. With further heating to higher temperatures, the deformation of the castable sample continued till reach the contraction value of −1.240% at a temperature 1450 °C where the castable sample is buckled. The fall in the strength of the castable sample B8 over 1200 °C is most likely due to the formation of a liquid phase as discussed before in this study. The softening temperature (T_a) of the loaded castable sample was found to be 1333 °C.

The castable sample B2 showed better behavior than the castable sample B8 (Fig. 7). Their RUL profiles suggest that during heating above 1200 °C up to 1400 °C a considerable amount of the liquid phase persisted and its viscosity probably decreased markedly over 1500 °C [17]. The poor RUL of tested castables at high temperature (above 1400 °C) was likely due to the reaction between the constituents of the castables matrix and the impurities from the bauxite aggregate that increases the fluidity of the formed liquid phase [18].

3.2.3. Slag-attack resistance

Slag-attack resistance test is performed to determine the rate of corrosion of a refractory material due to the physical and chemical action of slag or fired material in contact with it at service conditions. The slag used in this test is granulated blast-furnace slag (GBFS) supplied by Suez Cement Co., Suez, Egypt; its chemical composition is given in Table 5.

Photographed sections of the bauxite-based and kaolin-based castable samples containing spinel (preformed or in situ) after slag tests are shown in Figs. 8 and 10, respectively.

3.2.3.1. Bauxite-based castable samples. Fig. 8 shows the photographed sections of slag-corrosion and slag-penetration depths in bauxite-based castable samples (B0, B1, B2, B3, B7, B8 and B9).

The castable samples containing preformed spinel (B1, B2 and B3) and those containing in situ spinel (B7, B8 and B9) show a somewhat decrease in penetration by the molten slags as the spinel (preformed or in situ) content increases. The castable samples containing in situ spinel (B7, B8, and B9) show increased resistance to slag penetration compared to castable samples containing preformed spinel (B1, B2, and B3). In addition, the castable samples B1, B2, B3, B7, B8 and B9 show

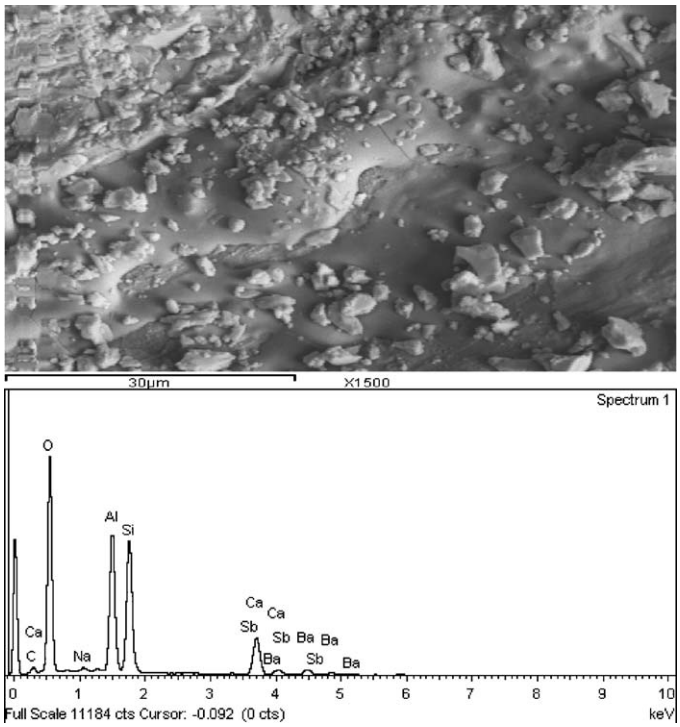

Fig. 9. SEM photomicrograph and EDX analysis of slag-attacked castable sample B2 fired at 1350 °C for 1 h.

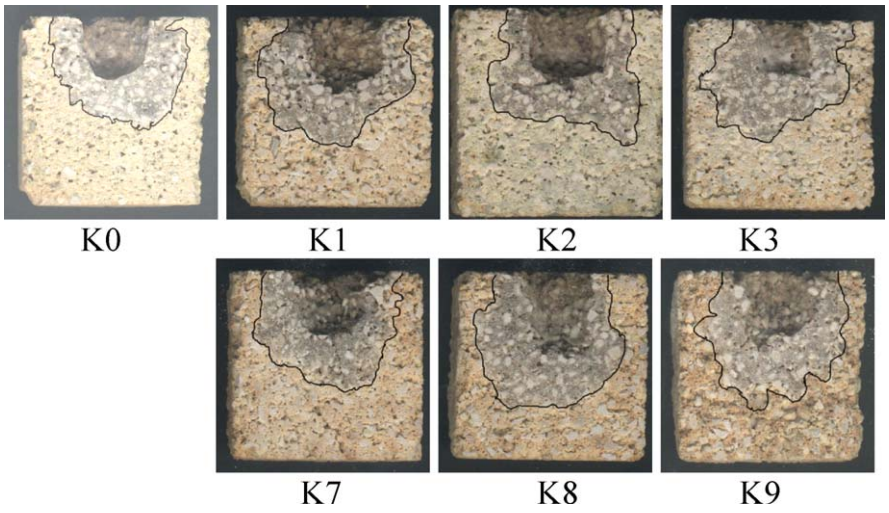

Fig. 10. Photographed sections of slag-corrosion and slag-penetration in bauxite-based castable samples (K0, K1, K2, K3, K7, K8 and K9).

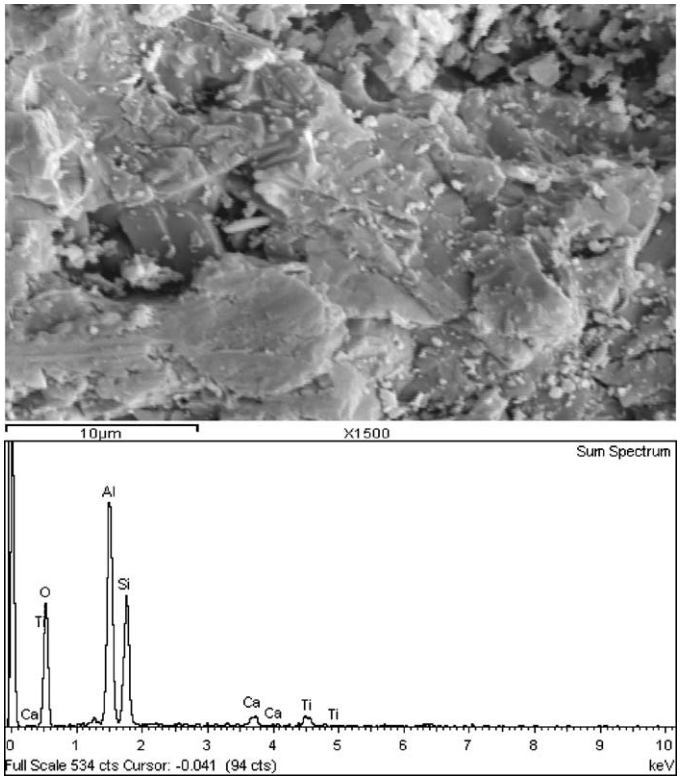

Fig. 11. SEM photomicrograph and EDX analysis of slag-attacked castable sample K2 fired at 1350 °C for 1 h.

a slight increase in corrosion by the molten slags as the spinel (preformed or in situ) content increases. Furthermore, the castable samples with in situ spinel (B7, B8, and B9) show a slight higher corrosion due to slag attack than those with preformed spinel (B1, B2, and B3) which did not show an obvious corrosion action. In other words, slag-corrosion and slag-penetration show opposite trends as the amount of spinel increases [19].

Fig. 9 shows the SEM micrograph of castable sample B2 which clearly indicates the low melting and detrimental C–A–S ($CaO–Al_2O_3–SiO_2$) phases existing in the microstructure matrix. The presence of these phases is confirmed by EDX analysis of the slag-attacked zone (Fig. 9).

3.2.3.2. Kaolin-based castable samples. Fig. 10 illustrates the photographed sections of slag-corrosion and slag-penetration depths in kaolin-based castable samples (K0, K1, K2, K3, K7, K8 and K9).

The castable samples containing preformed spinel (K1, K2, and K3) show penetration depths that are almost similar to those of castable samples containing in situ spinel (K7, K8, and K9). In addition, the castable samples containing preformed spinel (K1, K2 and K3) or in situ spinel (K7, K8 and K9) display a little increase in corrosion by the molten slag as spinel (preformed or in situ) content increases. Moreover, the castable samples with in situ spinel (K7, K8, and K9) display a little higher corrosion due to slag attack than those with preformed spinel (K1, K2, and K3).

Fig. 11 demonstrates the SEM photomicrograph and EDX analysis of castable sample K2. Obviously, the results of Fig. 11 displayed the appearance of the low melting and detrimental C–A–S phases existing in the microstructure matrix.

4. Conclusions

The main conclusions derived from this investigation are summarized as follows:

1. The XRD patterns of the bauxite-based castable samples indicated the formation of the corundum phase along with mullite phase in all of the specimens; while those of the kaolin-based castable samples showed that they composed mainly of transformed mullite phase along with some peaks characterizing the corundum phase.
2. The investigated castable samples showed characteristic positive PLC (expansion) and good volume stability as it showed a very small linear change (<1%). The castable samples containing in situ spinel showed higher PLC-values than those of the castable samples containing preformed spinel.

3. The RUL profiles for the two castable samples B2 and B8 were quite similar. They started softening at about 1300 °C followed by the rapid subsidence.
4. In general, the investigated castable samples showed a somewhat decrease in penetration by the molten slag and a slight increase in corrosion as the spinel (preformed or in situ) content increases. The castable samples containing in situ spinel showed an increase in resistance to slag-penetration and a slightly higher corrosion due to slag attack compared to castable samples containing preformed spinel.

References

[1] M. Zawrah, N. Khalil, Effect of mullite formation on properties of refractory castables, Ceram. Inter. 27 (6) (2001) 689–694.

[2] J. Yamada, S. Sakaki, K. Kasai, H. Ishimatsu, Application technology of monolithic refractories in NSC, in: Proceedings of (UNITECR'95), Kyoto, Japan, (1995), pp. 277–284.

[3] S. Mukhopadhyay, S. Ghosh, M. Mahapatra, R. Mazumder, P. Barick, S. Gupta, S. Chakraborty, Easy-to-use mullite and spinel sols as bonding agents in a high-alumina based ultra low cement castable, Ceram. Inter. 28 (7) (2002) 719–729.

[4] F. Ye, M. Rigaud, X. Liu, X. Zhong, High temperature mechanical properties of bauxite-based SiC-containing castables, Ceram. Inter. 30 (2004) 801–805.

[5] N. Khalil, Refractory concrete based on barium aluminate–barium zirconate cements for steel-making industries, Ceram. Inter. 31 (2005) 937–943.

[6] M. Zawrah, Effect of zircon additions on low and ultra-low cement alumina and bauxite castables, Ceram. Inter. 33 (5) (2007) 751–759.

[7] J. Garcia-Guinea, V. Correcher, J. Rubio, F. Valle-Fuentes, Effects of preheating on diaspore: modifications in color centers, structure and light emission, J. Phys. Chem. Solids (2005) 1–8.

[8] Y Chen, M. Wang, M. Hon, Secondary mullite formation in kaolin–Al_2O_3 ceramics, J. Mater. Res. 19 (3) (2004).

[9] S. Agathopoulos, H. Fernandes, D. Tulyaganov, J. Ferreira, Preparation of mullite whiskers from kaolinite using $CuSO_4$ as fluxing agent, Mater. Sci. Forum 455–456 (2004) 818–821.

[10] I. Štubňa, G. Varga, A. Trník, Investigation of kaolinite dehydroxylations is still interesting, Építôanyag 58, évf. 1, szám (2006).

[11] B. Myhre, B. Sandberg, A. Hundere, Castables with MgO–SiO_2–Al_2O_3 as bond phase, in: Presented at: the XXVI ALAFAR Congress in San Juan, Puerto Rico, 1997.

[12] S. Mukhopadhyay, S. Sen, T. Maiti, M. Mukherjee, R. Nandy, B. Sinhamahapatra, In situ spinel bonded refractory castable in relation to co-precipitation and sol–gel derived spinel forming agents, Ceram. Inter. 29 (8) (2003) 857–868.

[13] S. Ghosh, R. Majumdar, B. Sinhamahapatra, R. Nandy, M. Mukherjee, S. Mukhopadhyay, Micro structures of refractory castables prepared with sol gel additives, Ceram. Inter. 29 (6) (2003) 671–677.

[14] C. Ødegård, B. Myhre, N. Zhou, S. Zhang, Flow and properties of MgO based castables, in: Presented at XXXII ALAFAR Congress Antigua, Guatemala, 2004.

[15] C. Ødegård, H. Feldborg, B. Myhre, Mullite formation in refractory castables: the effect of fine and alusite in an alumina based ultra low cement castable, in: Presented at the XIII Conference on Refractory Castables, Prague, Czech, 2000.

[16] S. Kumar, S. Das, P. Daspoddar, Thermo-mechanical behavior of low cement castables derived from mullite aggregates synthesized from beach sand sillimanite, Ceram. Inter. 29 (2) (2003) 139–144.

[17] S. Chen, M. Cheng, S. Lin, Y. Ko, Thermal characteristics of Al_2O_3–MgO and Al_2O_3–spinel castables for steel ladles, Ceram. Inter. 28 (7) (2002) 811–817.

[18] H. Sarpoolaky, K. Ahari, W. Lee, Influence of in situ phase formation on microstructural evolution and properties of castable refractories, Ceram. Inter. 28 (5) (2002) 487–493.

[19] L. Diaz, R. Torrecillas, A.H. De Aza, P. Pena, Effect of spinel content on slag attack resistance of high alumina refractory castables, J. Eur. Ceram. Soc. 27 (16) (2007) 4623–4631.